applied optics

48 × 48 pixelated addressable full-color micro display based on flip-chip micro LEDs

YANG LI,[1,2] JIN TAO,[1] YONGZHOU ZHAO,[1,2] JIAXIAN WANG,[1,2] JINGUANG LV,[1] YUXIN QIN,[1] JINGQIU LIANG,[1,3] AND WEIBIAO WANG[1,4]

[1]State Key Laboratory of Applied Optics, Changchun Institute of Optics, Fine Mechanics and Physics, Chinese Academy of Sciences, Changchun, Jilin 130033, China
[2]University of Chinese Academy of Sciences, Beijing 100039, China
[3]e-mail: liangjq@ciomp.ac.cn
[4]e-mail: wangwb@ciomp.ac.cn

Received 15 August 2019; revised 29 September 2019; accepted 29 September 2019; posted 1 October 2019 (Doc. ID 375438); published 22 October 2019

This paper reports on the design and fabrication of a 48 × 48 full-color pixelated addressable light-emitting diode on silicon (LEDoS) micro display. The metallization pattern was designed and fabricated on a silicon substrate, while red, green, and blue monochromatic micro LEDs were integrated on the silicon substrate using transfer printing. The red, green, and blue micro LEDs are flip-chip structures in which red micro LEDs were fabricated using substrate transfer, mesa etching, metal deposition, and chip dicing. The integration process does not require wire bonding, which reduces the full-color pixel size and increases the integration speed. The LEDoS micro display can be addressed individually for each LED pixel and display representative patterns.

https://doi.org/10.1364/AO.58.008383

1. INTRODUCTION

LEDs have received wide attention due to their high brightness, good luminous efficiency, long lifetime, and wide color gamut [1–8]. Compared with liquid crystal displays (LCDs) and OLED displays, LED micro displays have a greater potential because of their self-illumination, good outdoor visibility, extreme environmental survivability, compact optical structure, and wide operating environment [9–11]. However, it is difficult to implement a full-color micro LED display, so most previous works have only discussed monochrome displays [12–18]. Regular three-color LEDs of red, green, and blue cannot usually be grown simultaneously on the same substrate. With a high indium doping, a new GaN epitaxial structure was designed and a multi-color display was realized by increasing the injection current and blue-shifting the emission wavelength [19]. However, this method still has some limitations regarding its color gamut. Applying phosphors or colloidal quantum dots to micro LEDs is another way to achieve full color on the same wafer, but this will cause a loss in efficiency, and the reliability has yet to be tested [20–23]. Therefore, it is reasonable to independently manufacture LEDs of three different colors and transfer them to a suitable substrate to form the display.

In 2014, Xue *et al.* designed and fabricated a 16 × 16 and 32 × 32 color-tunable addressable LED micro displays using chip-on-board (COB) technology with a full-color pixel size and pitch of 700 and 500 μm, respectively [24]. In 2015, Peng *et al.* used COB technology to design and manufacture a full-color pixelated addressable micro display on a transparent substrate with a full-color pixel pitch of 1 mm [25]. The COB is a mature discrete LED device packaging process that includes chip picking, pasting, and wire bonding. In 2016, Meitl *et al.* designed a special structure for micro LEDs with a gap underneath and a tether extending to the anchor of the wafer. The micro LEDs were then transferred from the wafer to the target substrate. After transfer printing, metal connections were formed using standard photolithography and reactive ion etching for the via holes, thereby realizing a 100 × 100 passively addressed micro LED display with a light-emitting area of 20 × 20 mm [26]. In 2017, Bower *et al.* used the same method and further transferred the micro ICs to realize a 44 × 44 active-addressing micro LED display with a full-color pixel size of 200 × 200 μm [27].

Transfer printing is the process of moving small components, such as micro LEDs or micro integrated circuits (ICs), from one substrate to another using a stamp [26–28]. Wire bonding is often required for conventional red LEDs since they are vertical structures; however, the wire bonding process is complicated and vulnerable and requires a relatively large space, which is disadvantageous to further reduce the full-color pixel size [24,25]. The aforementioned micro displays made with transfer printing often require specially designed micro LEDs and electrical connections after the transfer, which can realize high-resolution micro displays but are not conducive to mass production [26–28]. Therefore, we propose a full-color micro LED display by designing and manufacturing a silicon-based display substrate with a metallization pattern and transferring the flip-chip red, green, and blue micro LEDs onto the display substrate. In this method, wire bonding and special structured micro LEDs are not required, and thus the full-color pixel size is reduced and the integration speed is increased.

This paper reports the design and manufacture of a full-color LEDoS micro display. Red, green, and blue monochromatic micro LEDs were integrated on a pixelated addressable silicon substrate by transfer printing. The LEDoS micro displays have 48 × 48 × 3 (3 for RGB) pixels, a full-color pixel size of 250 × 480 μm, and a pitch of 500 μm on a single silicon substrate. The emission wavelengths of the LEDoS micro displays are 632.98, 514.56, and 463.72 nm, respectively. The LEDoS micro display can be used to form novel full-color displays for applications including augmented reality (AR), virtual reality (VR), head up display (HUD), and wearable displays with a high brightness and good visibility.

2. FLIP-CHIP MICRO LEDs

Red, green, and blue micro LEDs were used to realize a full-color micro LED displays. The green and blue micro LEDs were fabricated using a GaN-based multiple quantum well (MQW) LED structure grown on sapphire [29–33]. The epitaxial layer included an undoped GaN buffer layer (2.5 μm), a Si-doped n-type GaN layer (3 μm), a six-period InGaN/GaN MQW light-emitting layer, and a Mg-doped p-type GaN layer (120 nm). The p-GaN layer and the MQW active region were etched using inductively coupled plasma (ICP) dry etching until the n-GaN layer was exposed. An ITO layer was then deposited on the p-GaN layer to spread the current, and the wafer was rapidly thermally annealed in nitrogen to improve the Ohmic contact of the ITO with the GaN layer. A Cr/Au layer was deposited onto the wafer for n contact and p contact. The LED wafer was then diced into chips sized of 100 × 250 μm.

For the red micro LEDs, the epitaxial layer was grown on a GaAs substrate and transferred to a sapphire substrate following the process shown in Fig. 1. The epitaxial layer includes a Mg-doped n-type AlGaInP layer (2.5 μm), an AlGaInP/GaInP MQW active region, a Si-doped p-type AlGaInP layer (100 nm), and a GaP current spreading layer (8 μm). Since GaAs is electrically conductive and opaque, red micro LEDs are generally vertical structures. To fabricate flip-chip red micro LEDs, the GaP layer was first roughened and an Al_2O_3 film was deposited. The surface was then planarized with chemical mechanical polishing (CMP) and bonded to a transparent sapphire substrate under a high temperature and pressure. Finally, the GaAs substrate was removed using chemical etching to obtain an AlGaInP epitaxial wafer with a transparent sapphire substrate [17,34]. Thereafter, a process similar to green and blue micro LEDs was performed. An ICP dry etching was used to etch a n-type AlGaInP layer, and the MQW active region until the p-type AlGaInP layer was exposed. A Cr/Au layer was deposited for n contact and p contact, and the LED wafer was diced into chips of 100 × 250 μm. The red, green, and blue chips were all sapphire substrates and all flip-chip structures of the same size, which is beneficial for the subsequent integration processes.

3. DESIGN AND FABRICATION OF MICRO DISPLAY

The full-color display was designed and fabricated by integrating the red, green, and blue micro LEDs onto the display substrate, as shown in Fig. 2(a). The display has a 48 × 48 RGB micro LED array with a full-color pixel pitch of 500 μm and series pads surrounding the array. The series pads on each side of the array include VCC common anodes on the top of the array and red, green, and blue electrodes on the right, left, and bottom of the array, respectively. The series pads are connected to the control units with the micro LED array so the pixels in the array can be addressed individually through the control units. To form the electric connections before the integration, the display substrate with the metallization pattern was fabricated using standard photolithography and magnetron sputtering with a silicon wafer as a package substrate. The metallization pattern consisted of metal pads and wires with a pattern made from TiW/Au. As shown in Fig. 2(b), each pixel of the matrix is composed of red, green, and blue LED chips, and the arrangement of the metallization pads on the substrate coincides with the pads of the LED chips. In other words, the anode and cathode pads were fabricated on the silicon substrate to match the anode and cathodes of the LEDs. Moreover, the metal wires were designed

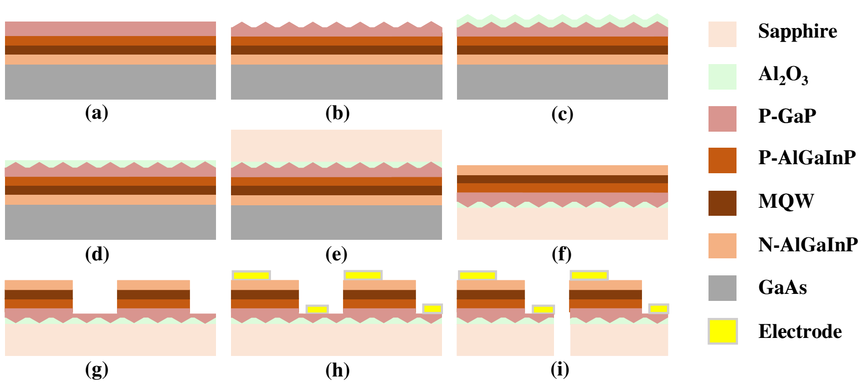

Fig. 1. (a) GaAs substrate epitaxial wafer, (b) GaP layer roughening, (c) Al_2O_3 film deposition, (d) CMP processing, (e) bonding with the sapphire substrate, (f) GaAs substrate removal, (g) ICP etching mesa, (h) metal deposition, and (i) micro LED dicing.

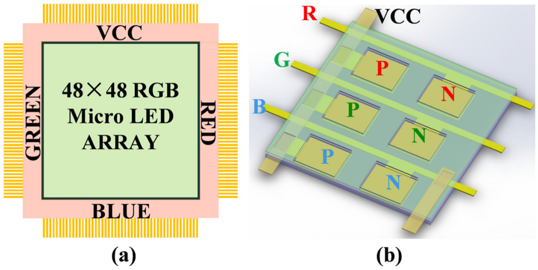

Fig. 2. (a) Structural diagram of the LEDoS micro display and (b) the pixel unit.

to control the micro LEDs in each pixel. To individually drive the micro LEDs, there were two metal wires for any micro LED: one for the anode and one for the cathode. The three micro LEDs for a single full-color pixel share the same anode metal wire. An extra metal wire is required for the blue micro LEDs in the same row to change the conduction direction of the cathode metal wire through the via hole. In summary, there were three anode pads, three cathode pads, and four or five metal wires for a single full-color pixel unit. The layout of the pads and metal wires is shown in Fig. 2(b).

As shown in Fig. 3(a), the micro LEDs in each column of the matrix are arranged in the order of red, green, and blue. Each row of the matrix is one of red, green, and blue micro LEDs. The anodes of the micro LEDs in the same column are connected together, and each column is connected to the corresponding VCC series pads above the matrix. The LEDs of the same row have the same color, and the cathodes for the red, green, and blue LEDs in the same row are connected together. Each row of the green and red LEDs are connected to the series pads corresponding to the left and right sides of the matrix, respectively, while each row of the blue LEDs is connected from the horizontal direction to the vertical direction through the via hole and to the corresponding series pads below the matrix. As distinct from the VCC, red and green series pads, the leftmost blue series pad controls the bottom row of blue LEDs, the rightmost blue series pad controls the top row of blue LEDs, and so on.

The fabrication process to manufacture the display substrate with the metallized pattern is explained below and shown in Fig. 3(b). First, a silicon wafer with a 2 μm thick oxide layer was prepared. A 300 nm TiW/Au layer was grown on the wafer using magnetron sputtering, and the LED pads and lateral wires (20 μm width) were formed with photolithography. Next, a 500 nm SiO_2 isolation layer was grown using plasma enhanced chemical vapor deposition (PECVD), and the via holes served as the interconnection contact region, which were exposed by applying ICP etching. Then, the vertical wires (40 μm width) were formed using photolithography after a 700 nm TiW/Au layer was grown on the wafer, which was followed by the deposition of a 1000 nm SiO_2 passivation layer. Finally, p and n pads were exposed by removing the excessive passivation layer for the connection with the LED pads. The substrate for the display with the metallization pattern is shown in Fig. 4(a).

After the metallized pattern was fabricated, low-melting-point solder (LMPS; melting point: 47°C, composition: Sn 8.3%, Bi 44.7%, Pb 22.6%, Cd 5.3%, In 19.1%) was employed to the pads of the display substrate [35]. Then a polydimethylsiloxane (PDMS) stamping sheet with convex patterns was used to selectively pick up the micro LEDs from the donor substrate with a relatively high peel velocity [36]. The micro LEDs on the donor substrate were arranged by the pick-and-place process, respectively. After the pick-up process, the micro LEDs were placed in contact with the pads of the display substrate at 60°C. Subsequently, the LMPS solidified at room temperature, and the PDMS stamping sheet was peeled off. The micro LEDs were

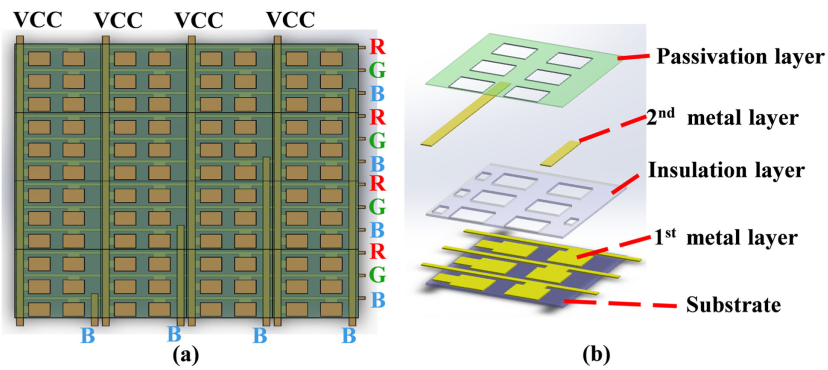

Fig. 3. (a) Structure diagram of the display substrate and (b) the structure of the pixel unit.

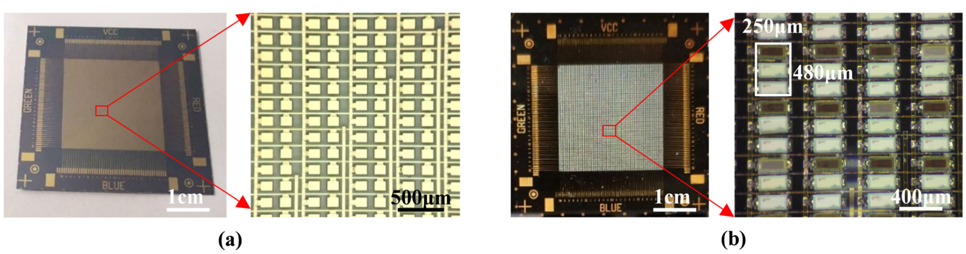

Fig. 4. (a) Substrate for the LEDoS micro display and (b) photograph of the LEDoS micro display.

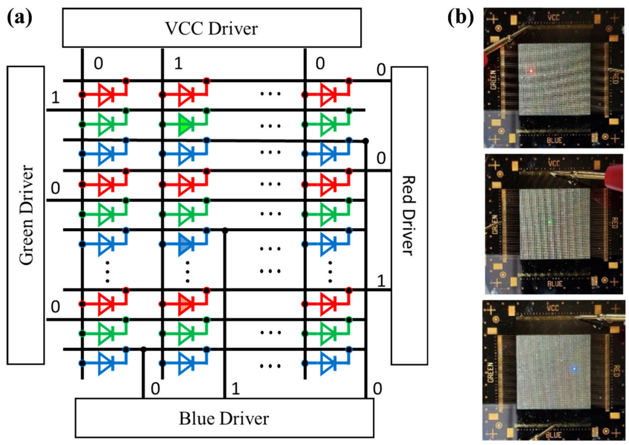

Fig. 5. (a) Schematic of the driving circuit for the LEDoS micro display and (b) the individual illumination of red, green, and blue micro LEDs.

thus transferred to the display substrate. The display substrate was then thermally annealed at 80°C [35,36]. The surface tension of the solder causes it to spontaneously move to the metal pads to pull the offset micro LEDs back to their specified positions. Thus, the micro LEDs formed a firm connection with the substrate to finally obtain the full-color self-illumination matrix shown in Fig. 4(b). Wire bonding is often required when the red LED is of the vertical type. Wire bonding is time consuming because each vertical micro LED needs to connect its p-pad of the display substrate with the metal wire after the LED has been placed on the cathode pad of the substrate. In contrast, transfer printing can integrate multiple micro LEDs into the display substrate at one time. The red, green, and blue micro LEDs are all flip-chips of the same size. Therefore, for individual micro LEDs, the integration process can be seen as flip-chip bonding. Compared with wire bonding, flip-chip bonding has better connections to the display substrate because the wires are vulnerable to breakage. To form the connections with the vertical LEDs, an anode pad needs to be designed near the LED, while for a flip-chip LED, the anode pad is designed under the LED to reduce the full-color pixel size.

The full-color display is driven passively. The anode of each column of the LEDs is connected to the column scan line, and the cathode of each row of LEDs is connected to the row scan line. The red, green, and blue LEDs are each connected to different scan lines. The common anode lines are led to the VCC driver above the array, and the red and green scan lines are led to the red and green drivers on the right and left sides of the array, respectively. The blue scan lines are led to the blue drivers below the array through the via holes. When a particular Xth column scan and Yth line scan are gated, the LED pixels at the intersection (X, Y) are illuminated. As shown in Fig. 5, the red micro LED (9,18), the green micro LED (21,23), and the blue micro LED (38,22) were illuminated individually.

4. RESULTS AND DISCUSSION

Photoelectric performance tests were performed on the prepared full-color micro LED display. Figure 6(a) shows a schematic diagram of the test system. The micro display was placed on the probe station, the voltage and current of the micro LED were changed and measured using the ITECH DC Source Meter, the light output power of the micro LED was measured with the CNI Laser Power Meter, and the spectrum of the micro LED was measured in the Ocean Optics USB4000. Figure 6(b) shows the red, green, and blue micro LEDs that were individually lit.

Figures 7(a)–7(c) show the current versus voltage (I-V) and optical power versus voltage (L-V) characteristics of the red, green, and blue LEDs in a typical full-color pixel that is DC biased at room temperature. The forward turn-on voltages of the RGB LEDs are 1.7, 2.3, and 2.5 V, respectively. As the voltage increases, the output optical power of the LED first increases and then decreases, which shows a droop phenomenon that can be contributed to an increased non-radiative recombination that is stronger than that of the radiative recombination when the injection current increases at high current [37–39]. The maximum light output powers for the red, green, and blue LEDs are 0.68, 1.55, and 3.77 mW, respectively. Figure 7(d) shows the emission wavelength spectrum for the red, green, and blue LEDs at an operating current of 20 mA. The center wavelengths of the LEDoS micro display are 632.98, 514.56, and 463.72 nm, respectively. Their full width at half-maximums are 20, 25, and 30 nm, respectively.

For passive drive mode displays, it is necessary to evaluate the effects of the series resistance for the address lines on the optoelectronic performance of each pixel. Equations (1)–(3) are used to determine the series resistance of the micro LEDs in the matrix from the pixel resistance of the micro LED, the distance from the VCC driver, and the distance from the red, green, and blue drivers, as follows:

$$R_R = R_{Rp} + R_r \times (48 - m) + R_c \times (n - 1), \qquad \textbf{(1)}$$

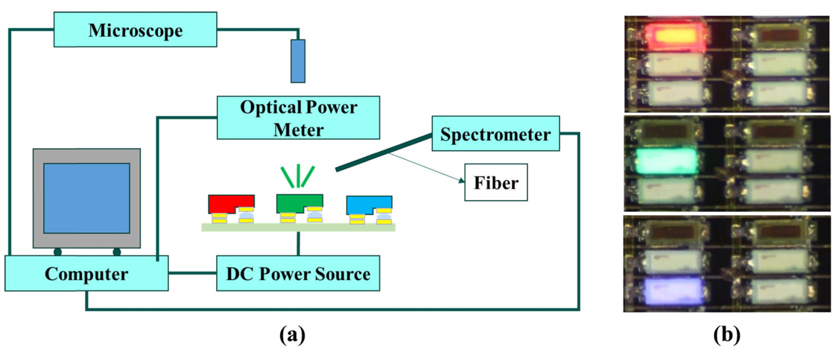

Fig. 6. (a) Schematic diagram of the photoelectric performance test system and (b) the individually illuminated micro LEDs.

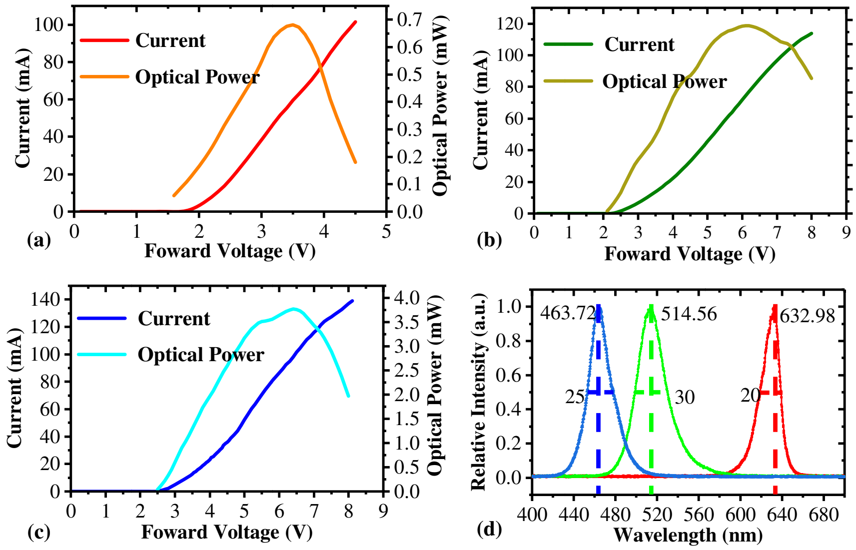

Fig. 7. I-V and L-V characteristics for the (a) red, (b) green, and (c) blue micro LEDs. (d) The spectrum for the red, green, and blue LEDs at an operating current of 20 mA.

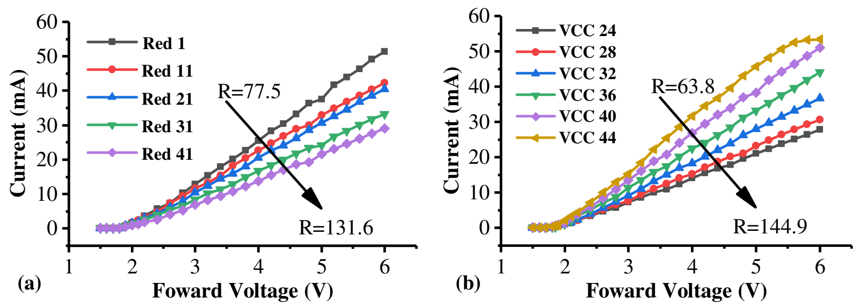

Fig. 8. I-V curves for the red pixels of a single (a) column and (b) row.

$$R_G = R_{Gp} + R_r \times (m-1) + R_c \times (n-1), \tag{2}$$

$$R_B = R_{Bp} + R_r \times |48 - m - n| + R_c \times 48. \tag{3}$$

Here R_R, R_G, and R_B are the series resistances for the red, green, and blue micro LEDs in the matrix; the R_{Rp}, R_{Gp}, and R_{Bp} are the pixel resistances of the red, green, and blue micro LEDs; R_r is the line resistance between two LEDs in each row; R_c is the line resistance between two LEDs in each column, and m and n are the number of pixels on the row and column, respectively. For the red micro LEDs, the driver is on the right of the matrix. When m increases, the distance between the pixel and the driver is reduced; however, for the green micro LEDs, the distance increases because the green driver is located on the left of the matrix. For both red and green micro LEDs, the distance between the pixel and the VCC driver increases with n. However, unlike the red and green micro LEDs, the blue driver is situated below the matrix, and vertical metal wires are used to attach the driver with the horizontal metal wires connected the cathode for the blue micro LEDs along the same row through the via holes. The vertical metal wires have the same width and thickness as the VCC metal wires, and their lengths increase as n increases. Therefore, for any blue micro LED, the sum of

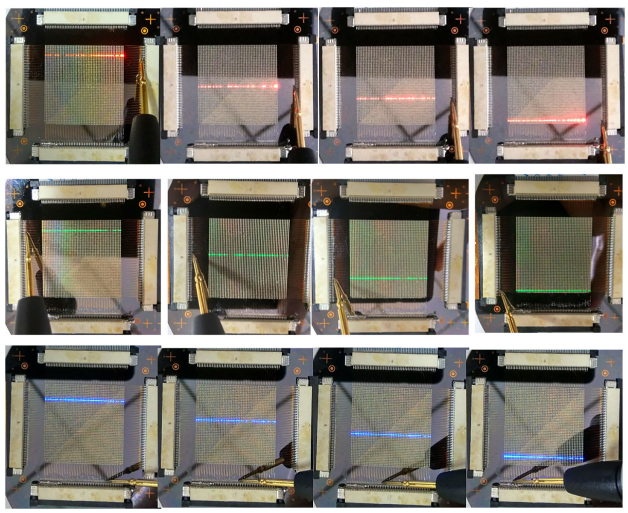

Fig. 9. Display results of single-row illumination scans for the LEDoS micro display.

the distance between the anode of the blue LED and the VCC driver and the distance between the via hole and the blue driver is always the same. Therefore, the series resistance of the blue

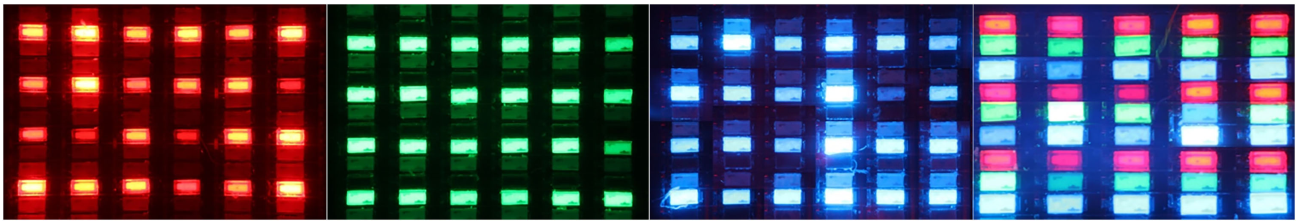

Fig. 10. Images of R, G, B and full-color illuminated micro LED arrays.

micro LEDs depends on the distance between the blue LED and the via hole in the same row. The farther the pixel is from the drivers, the longer the conduction path and the higher the series resistance. The brightness of the LED depends on the drive current. A larger series resistance causes a smaller drive current, which decreases the brightness of the display pixels.

The electrical performance of the 48 × 48 micro LED display array was analyzed, because the brightness uniformity of each LED is an important factor in display applications. Taking the red micro LEDs as an example, the LED I-V characteristics were measured for each pixel on a single column as shown in Fig. 8(a). It was found that as n increased from 1 to 41, the series resistance of the pixel increased from 77.5 to 131.6 Ω. In addition, the I-V characteristic of the LEDs for each pixel on a single row was measured as shown in Fig. 8(b). Since the red light driver is located on the right side of the display, as m increased from 24 to 44, the series resistance for the pixel reduced from 144.9 to 63.8 Ω. The trends of the pixel series resistance for the red micro LEDs are consistent with Eq. (1). Changes in the row line resistance were found to be greater than those for the column. This can be attributed to differences between the row line thickness (300 nm) and the column line thickness (700 nm) and differences between the line width (20 μm) and the column line width (40 μm). That is, larger line thicknesses and widths cause smaller resistances.

Figure 9 shows the LEDoS micro display for red, green, and blue colors that scan the entire array at the specific voltage of 2.75 V from the top to the bottom, which gives a relatively high yield. Figure 10 shows partial red, green, and blue LEDs lit up both individually and simultaneously. There is an uneven brightness, which is mainly due to the poor contact between the micro LEDs and the pads on the display substrate. Uneven brightness can be eliminated in future work using a point-by-point correction and the application of a constant current driver.

The design and manufacturing method reported in this paper is based on flip-chip red AlGaInP micro LEDs. Under the same injection current, flip-chip red LEDs have a higher output power than vertical red LEDs of equal size. The flip-chip red micro LED light-emitting surface is on the sapphire side, which is colorless and transparent. The inner light of the quantum well layer can be emitted from the entire surface, but vertical red micro LEDs have an anode pad in the middle of the light-emitting surface, which causes a considerable loss in the output light intensity. The vertical red micro LED substrate is GaAs, so its parasitic resistance is large, and the thermal energy conversion during operation is high. Therefore, there are more non-radiative recombination centers inside the device well layer, which results in a decreased proportion of photons generated by the chip radiation recombination. Therefore, the electro-optic conversion efficiency of vertical LEDs is lower than that of a flip-chip LED. Compared with the vertical LED, the flip-chip LED does not require wire bonding, and thus it has a faster integration speed, better connection with the display substrate, and a greater pixel reduction potential.

The full-color display was fabricated by integrating the flip-chip micro LEDs with the metallized display substrate through transfer printing. The metallized display substrate was silicon based and fabricated using semiconductor processing, which improves the display resolution and mass production. Moreover, a special structure of micro LEDs is not required with this process. The proposed method is also more efficient compared with the processing of forming the electrical connections after the transfer. The pixels are 480 × 250 μm with a pitch of 500 μm. The resolution of the micro LED display can increase by further reducing the size of the LEDs and optimizing the driving substrate layout.

5. CONCLUSIONS

In this paper, flip-chip red AlGaInP micro LEDs with the same size as the blue and green GaN micro LEDs was prepared using a substrate transfer process. A pixelated addressable full-color LEDoS micro display was designed and fabricated using transfer printing on a metallized silicon substrate. The full-color LEDoS micro display had a high brightness and good pixel controllability, indicating it has great potential for both indoor and outdoor applications. Full-color LEDoS micro displays have the potential for a further increased resolution due to flip-chip red LEDs and the transfer printing.

Funding. Science and Technology Planning Project of Guangdong Province (2016B010111003); Science and Technology Development Plan of Jilin Province (20180201024GX, 20190302062GX); National Key Research and Development Program of China (2018YFB1801900).

REFERENCES

1. E. F. Schubert, J. K. Kim, H. Luo, and J. Q. Xi, "Solid-state lighting—a benevolent technology," Rep. Prog. Phys. **69**, 3069–3099 (2006).
2. H. X. Jiang and J. Y. Lin, "Nitride micro-LEDs and beyond—a decade progress review," Opt. Express **21**, A475–A484 (2013).
3. J. H. Oh, S. J. Yang, and Y. R. Do, "Healthy, natural, efficient and tunable lighting: four-package white LEDs for optimizing the circadian effect, color quality and vision performance," Light Sci. Appl. **3**, e141 (2014).

4. T. Pulli, T. Dönsberg, T. Poikonen, F. Manoocheri, P. Kärhä, and E. Ikonen, "Advantages of white LED lamps and new detector technology in photometry," Light Sci. Appl. **4**, e332 (2015).
5. G. Lozano, S. R. K. Rodriguez, M. A. Verschuuren, and J. G. Rivas, "Metallic nanostructures for efficient LED lighting," Light Sci. Appl. **5**, e16080 (2016).
6. Y. Peng, R. Li, H. Cheng, Z. Chen, H. Li, and M. Chen, "Facile preparation of patterned phosphor-in-glass with excellent luminous properties through screen-printing for high-power white light-emitting diodes," J. Alloys Compd. **693**, 279–284 (2017).
7. H. Wang, Y. Mou, Y. Peng, J. Liu, R. Liang, M. Chen, J. Dai, and C. Chen, "White light-emitting diodes with high color quality fabricated using phosphor-in-glass integrated with liquid-type quantum dot," IEEE Electron Dev. Lett. **40**, 601–604 (2019).
8. Y. Peng, Y. Mou, Q. Sun, H. Cheng, M. Chen, and X. Luo, "Facile fabrication of heat-conducting phosphor-in-glass with dual-sapphire plates for laser-driven white lighting," J. Alloys Compd. **790**, 744–749 (2019).
9. H. X. Jiang, S. X. Jin, J. Li, J. Shakya, and J. Y. Lin, "III-nitride blue microdisplays," Appl. Phys. Lett. **78**, 1303–1305 (2001).
10. H. W. Choi, C. W. Jeon, M. D. Dawson, S. Member, P. R. Edwards, and R. W. Martin, "Fabrication and performance of parallel-addressed InGaN micro-LED arrays," IEEE Photon. Technol. Lett. **15**, 510–512 (2003).
11. H.-W. Chen, J.-H. Lee, B.-Y. Lin, S. Chen, and S.-T. Wu, "Liquid crystal display and organic light-emitting diode display: present status and future perspectives," Light Sci. Appl. **7**, 17168 (2018).
12. Z. J. Liu, K. M. Wong, C. W. Keung, C. W. Tang, and K. M. Lau, "Monolithic LED microdisplay on active matrix substrate using flip-chip technology," IEEE J. Sel. Top. Quantum Electron. **15**, 1298–1302 (2009).
13. J. Day, J. Li, D. Y. C. Lie, C. Bradford, J. Y. Lin, and H. X. Jiang, "III-Nitride full-scale high-resolution microdisplays," Appl. Phys. Lett. **99**, 031116 (2011).
14. J. Day, J. Li, D. Y. C. Lie, C. Bradford, J. Y. Lin, and H. X. Jiang, "Full-scale self-emissive blue and green microdisplays based on GaN micro-LED arrays," Proc. SPIE **8268**, 82681X (2012).
15. Z. J. Liu, W. C. Chong, K. M. Wong, and K. M. Lau, "360 PPI flip-chip mounted active matrix addressable light emitting diode on silicon (LEDoS) micro-displays," J. Disp. Technol. **9**, 678–682 (2013).
16. X. Bao, J. Liang, Z. Liang, W. Wang, C. Tian, Y. Qin, and J. Lü, "Design and fabrication of AlGaInP-based micro-light-emitting-diode array devices," Opt. Laser Technol. **78**, 34–41 (2016).
17. R.-H. Horng, H.-Y. Chien, F.-G. Tarntair, and D.-S. Wuu, "Fabrication and study on red light micro-LED displays," IEEE J. Electron Dev. Soc. **6**, 1064–1069 (2018).
18. C. J. Chen, H. C. Chen, J. H. Liao, C. J. Yu, and M. C. Wu, "Fabrication and characterization of active-matrix 960×540 blue GaN-based micro-LED display," IEEE J. Quantum Electron. **55**, 1–6 (2019).
19. S. Zhang, Z. Gong, J. J. D. McKendry, S. Watson, A. Cogman, E. Xie, P. Tian, E. Gu, Z. Chen, G. Zhang, A. E. Kelly, R. K. Henderson, and M. D. Dawson, "CMOS-controlled color-tunable smart display," IEEE Photon. J. **4**, 1639–1646 (2012).
20. Z. J. Liu, K. M. Wong, W. C. Chong, and K. M. Lau, "P-34: active matrix programmable monolithic light emitting diodes on silicon (LEDoS) displays," SID Int. Symp. Dig. Tech. Pap. **42**, 1215–1218 (2011).
21. H. V. Han, H. Y. Lin, C. C. Lin, W. C. Chong, J. R. Li, K. J. Chen, P. Yu, T. M. Chen, H. M. Chen, K. M. Lau, and H. C. Kuo, "Resonant-enhanced full-color emission of quantum-dot-based micro LED display technology," Opt. Express **23**, 32504–32515 (2015).
22. B. H. Kim, M. S. Onses, J. B. Lim, S. Nam, N. Oh, H. Kim, K. J. Yu, J. W. Lee, J. H. Kim, S. K. Kang, C. H. Lee, J. Lee, J. H. Shin, N. H. Kim, C. Leal, M. Shim, and J. A. Rogers, "High-resolution patterns of quantum dots formed by electrohydrodynamic jet printing for light-emitting diodes," Nano Lett. **15**, 969–973 (2015).
23. H.-C. Lin, C. W. Sher, D. H. Hsieh, X. Y. Chen, H. M. P. Chen, T. M. Chen, K. M. Lau, C. H. Chen, C. C. Lin, and H. C. Kuo, "Optical cross-talk reduction in a quantum-dot-based full-color micro-light-emitting-diode display by a lithographic-fabricated photoresist mold," Photon. Res. **5**, 411–416 (2017).
24. B. Xue, H. Yang, F. Yu, X. Wang, L. Liu, Y. Pei, P. Lu, H. Xie, Q. Kong, J. Li, X. Yi, J. Wang, and J. Li, "Colour tuneable micro-display based on LED matrix," Proc. SPIE **9270**, 92701B (2014).
25. D. Peng, K. Zhang, V. S.-D. Chao, W. Mo, K. M. Lau, and Z. Liu, "Full-color pixelated-addressable light emitting diode on transparent substrate (LEDoTS) micro-displays by CoB," J. Disp. Technol. **12**, 742–746 (2016).
26. M. Meitl, E. Radauscher, S. Bonafede, D. Gomez, T. Moore, C. Prevatte, B. Raymond, B. Fisher, K. Ghosal, A. Fecioru, A. J. Trindade, D. Kneeburg, and C. A. Bower, "55-1: invited paper : passive matrix displays with transfer-printed microscale inorganic LEDs," SID Int. Symp. Dig. Tech. Pap. **47**, 743–746 (2016).
27. A. Meitl, B. Ra, J. Trin, A. Bower, M. A. Meitl, E. Radauscher, R. Rotzoll, B. Raymond, S. Bonafede, D. Gomez, T. Moore, C. Prevatte, A. Fecioru, A. J. Trindade, and C. A. Bower, "19-4: invited paper: emissive displays with transfer-printed microscale inorganic LEDs," SID Int. Symp. Dig. Tech. Pap. **48**, 257–263 (2017).
28. C. A. Bower, M. A. Meitl, B. Raymond, E. Radauscher, R. Cok, S. Bonafede, D. Gomez, T. Moore, C. Prevatte, B. Fisher, R. Rotzoll, G. A. Melnik, A. Fecioru, and A. J. Trindade, "Emissive displays with transfer-printed assemblies of $8\ \mu m \times 15\ \mu m$ inorganic light-emitting diodes," Photon. Res. **5**, A23–A29 (2017).
29. X. Liu, S. Zhou, Y. Gao, H. Hu, Y. Liu, C. Gui, and S. Liu, "Numerical simulation and experimental investigation of GaN-based flip-chip LEDs and top-emitting LEDs," Appl. Opt. **56**, 9502–9509 (2017).
30. S. Zhou, C. Zheng, J. Lv, Y. Gao, R. Wang, and S. Liu, "GaN-based flip-chip LEDs with highly reflective ITO/DBR p-type and via hole-based n-type contacts for enhanced current spreading and light extraction," Opt. Laser Technol. **92**, 95–100 (2017).
31. S. Zhou, X. Liu, Y. Gao, Y. Liu, M. Liu, Z. Liu, C. Gui, and S. Liu, "Numerical and experimental investigation of GaN-based flip-chip light-emitting diodes with highly reflective Ag/TiW and ITO/DBR Ohmic contacts," Opt. Express **25**, 26615–26627 (2017).
32. B. Tang, J. Miao, Y. Liu, H. Wan, N. Li, S. Zhou, and C. Gui, "Enhanced light extraction of flip-chip mini-LEDs with prism-structured sidewall," Nanomaterials **9**, 1–8 (2019).
33. S. Zhou, X. Liu, H. Yan, Z. Chen, Y. Liu, and S. Liu, "Highly efficient GaN-based high-power flip-chip light-emitting diodes," Opt. Express **27**, A669–A692 (2019).
34. F.-L. Wu, S.-L. Ou, Y.-C. Kao, C.-L. Chen, M.-C. Tseng, F.-C. Lu, M.-T. Lin, and R.-H. Horng, "Thin-film vertical-type AlGaInP LEDs fabricated by epitaxial lift-off process via the patterned design of Cu substrate," Opt. Express **23**, 18156–18165 (2015).
35. H. Onoe, A. Nakai, E. Iwase, K. Matsumoto, and I. Shimoyama, "Temperature-controlled transfer and self-wiring for multi-color light-emitting diode arrays," J. Micromechan. Microeng. **19**, 075015 (2009).
36. M. A. Meitl, Z. T. Zhu, V. Kumar, K. J. Lee, X. Feng, Y. Y. Huang, I. Adesida, R. G. Nuzzo, and J. A. Rogers, "Transfer printing by kinetic control of adhesion to an elastomeric stamp," Nat. Mater. **5**, 33–38 (2006).
37. P. Tian, J. J. D. Mckendry, J. Herrnsdorf, S. Watson, R. Ferreira, I. M. Watson, E. Gu, A. E. Kelly, and M. D. Dawson, "Temperature-dependent efficiency droop of blue InGaN micro-light emitting diodes," Appl. Phys. Lett. **105**, 171107 (2014).
38. D. S. Meyaard, Q. Shan, J. Cho, E. F. Schubert, S. H. Han, M. H. Kim, C. Sone, S. J. Oh, and J. K. Kim, "Temperature dependent efficiency droop in GaInN light-emitting diodes with different current densities," Appl. Phys. Lett. **100**, 081106 (2012).
39. J. Piprek, "Efficiency droop in nitride-based light-emitting diodes," Phys. Status Solidi Appl. Mater. Sci. **207**, 2217–2225 (2010).